

**Revista Mexicana de  
Astronomía y Astrofísica**

Revista Mexicana de Astronomía y Astrofísica

ISSN: 0185-1101

rmaa@astroscu.unam.mx

Instituto de Astronomía

México

Hildebrand, R. H.; Vaillancourt, J. E.  
MAGNETIC FIELDS AND POLARIZED EMISSION FROM SELECTED ENVIRONMENTS  
Revista Mexicana de Astronomía y Astrofísica, vol. 36, 2009, pp. 137-141  
Instituto de Astronomía  
Distrito Federal, México

Available in: <http://www.redalyc.org/articulo.oa?id=57115743020>

- How to cite
- Complete issue
- More information about this article
- Journal's homepage in redalyc.org

redalyc.org

Scientific Information System

Network of Scientific Journals from Latin America, the Caribbean, Spain and Portugal

Non-profit academic project, developed under the open access initiative

## MAGNETIC FIELDS AND POLARIZED EMISSION FROM SELECTED ENVIRONMENTS

R. H. Hildebrand<sup>1</sup> and J. E. Vaillancourt<sup>2</sup>

### RESUMEN

Medidas de la emisión polarizada de las nubes moleculares han producido mapas de los campos magnéticos proyectados en el cielo. El espectro de polarización ha provisto evidencia de componentes múltiples en nubes en las cuales los granos de polvo a diferentes temperaturas tienen diferentes eficiencias de polarización. Con las mejoras en la resolución angular y con la selección adicional de longitudes de onda, está siendo posible hacer observaciones en entornos selectos tales como grumos densos, cúmulos de estrellas embebidas, y regiones de alta densidad en columna. Estas observaciones proveen modelos de nubes mejorados y también proveen de pruebas para los mecanismos de alineamiento de granos tales como el alineamiento por torcas radiativas. Medidas de la dispersión del campo, aplicadas a estudios de las intensidades de los campos o a la turbulencia, requieren resolución angular alta, y medidas precisas del ángulo de posición en muchos puntos. Las posibilidades para tales medidas, especialmente en el rango  $\sim 50 - 200 \mu\text{m}$ , serán realizadas enormemente cuando SOFIA esté equipada con un polarímetro de alto rendimiento en el lejano infrarrojo.

### ABSTRACT

Measurements of polarized emission from molecular clouds have provided maps of magnetic fields as projected on the sky. The polarization spectrum has given evidence for multiple cloud components in which dust grains at different temperatures have different polarizing efficiencies. With improvements in angular resolution and with additional choices of wavelength, it is becoming possible to make observations in selected environments such as dense clumps, clusters of embedded stars, and regions of high column densities. These observations provide improved cloud models and also provide tests of grain alignment mechanisms such as alignment by radiative torques. Measurements of field dispersion, as applied to studies of field strengths or turbulence, require high angular resolution, and accurate position angle measurements at very many points. The possibilities for such measurements, especially in the range  $\sim 50 - 200 \mu\text{m}$ , will be greatly enhanced when SOFIA is equipped with a high-performance far-infrared polarimeter.

*Key Words:* ISM: dust, extinction — ISM: clouds — ISM: magnetic fields — polarization

### 1. INTRODUCTION

Well-known maps of starlight polarization (e.g., Mathewson & Ford 1970; Heiles 2000) have shown that the magnetic field in the tenuous environment along lines of sight to stars lies close to the Galactic plane. The few polarization vectors steeply inclined to the plane disappear if one selects only vectors toward distant stars (Figure 1).

By contrast, maps of polarized emission from individual molecular clouds at far-IR and submillimeter wavelengths show little or no relationship to the Galactic plane (Figure 1).

Within the clouds, one finds structure associated with processes such as expanding H II regions, differential rotation, or gravitational collapse. By combining flux maps, polarimetric maps, and ion and neutral molecular line width measurements, it is becoming possible to model 3-D magnetic field and mass distributions. A model for the molecular cloud DR 21 Main (Kirby 2009), indicates a collapsing core where the gravitational potential dominates over magnetic support within a radius of  $\sim 1$  pc (Figure 2).

### 2. DUST ENVIRONMENTS

Characteristics of the environment that influence polarized emission include temperature structure, inclination to the line of sight, opacity, and exposure to radiation from embedded stars or the interstellar radiation field, all effects that bear on the polarization spectrum (Figure 3). A new result is a compar-

<sup>1</sup>Enrico Fermi Institute and Departments of Physics and Astronomy & Astrophysics, University of Chicago, 5640 S. Ellis Ave., Chicago, IL 60637 USA (roger@oddjob.uchicago.edu).

<sup>2</sup>Division of Physics, Mathematics, & Astronomy, Caltech, 1200 E. California Blvd., MS 320-47, Pasadena, CA 91125 USA (johnv@submm.caltech.edu).

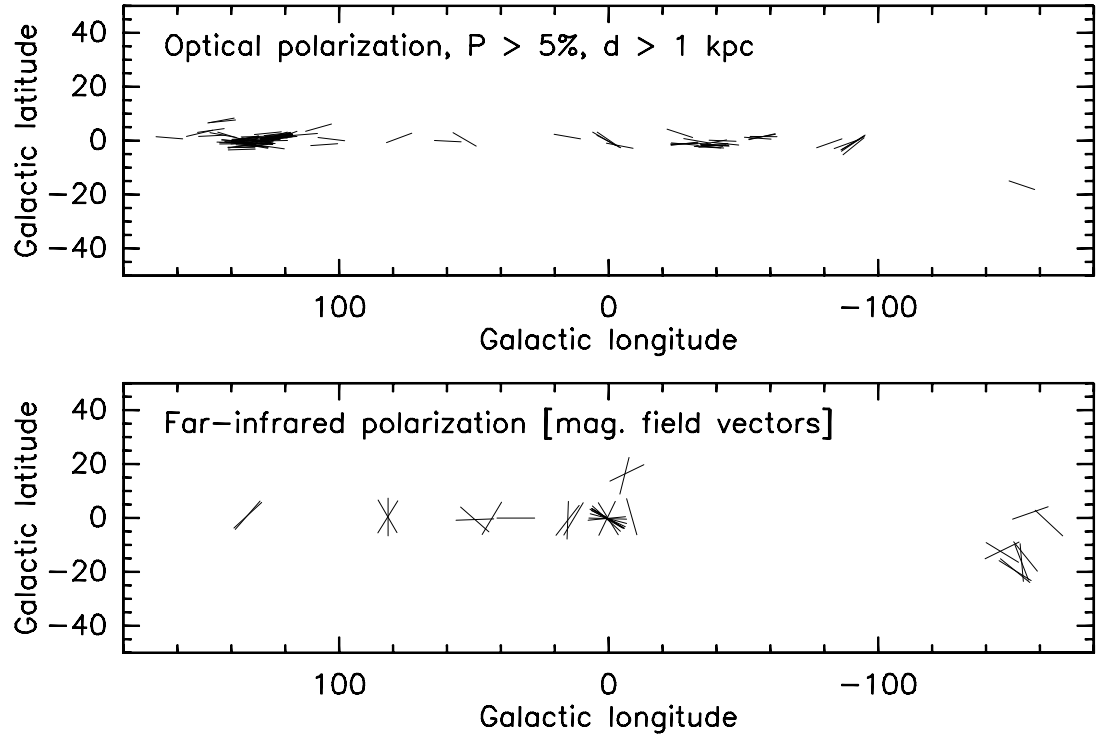


Fig. 1. *Top*: Galactic polarization measurements of the diffuse ISM at optical wavelengths (Heiles 2000). *Bottom*: Mean field direction for 27 Galactic molecular clouds observed in the far-infrared and submillimeter (Hildebrand 2002; courtesy C. D. Dowell).

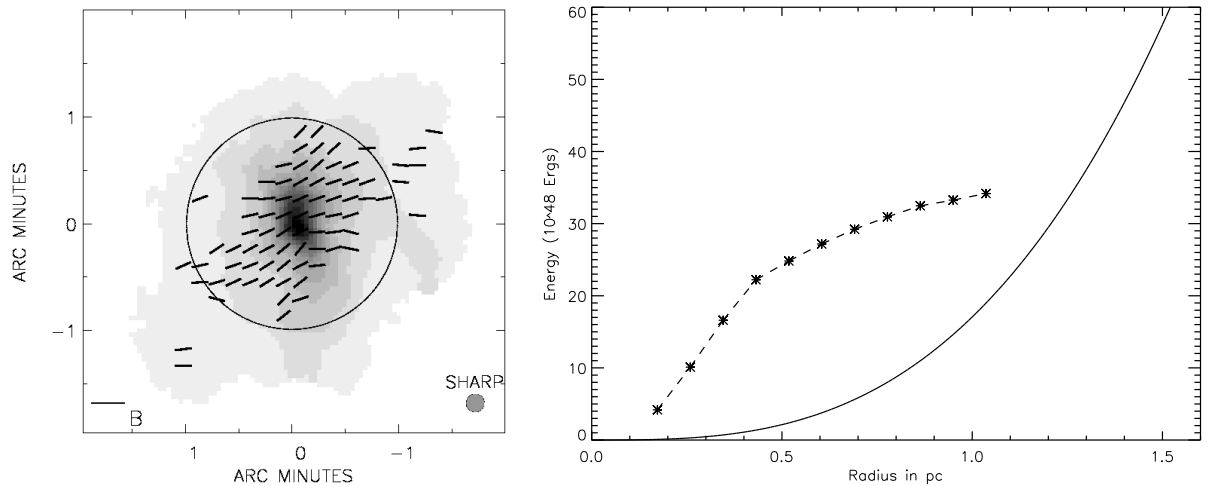


Fig. 2. DR 21 (Main). *Left*: Magnetic field vectors. Circle shows radius within which the gravitational field is dominant. *Right*: Magnetic potential energy (solid curve) and gravitational potential energy (dashed curve) vs. radius (Kirby 2009).

ison of degrees of polarization at  $350 \mu\text{m}$  and  $450 \mu\text{m}$  for measurements outside the central core of a cloud (Figures 4 and 5; Vaillancourt et al. 2008).

Our interpretation is that the dust exposed to radiation from embedded stars is warmer and better aligned (Hildebrand et al. 1999). The effect of

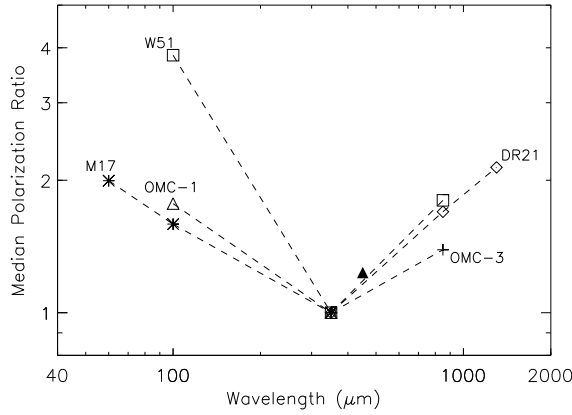


Fig. 3. Far-infrared and submillimeter polarization spectrum, normalized at  $350\ \mu\text{m}$  (Vaillancourt et al. 2008). The solid triangle is from the new data shown in Figure 5.

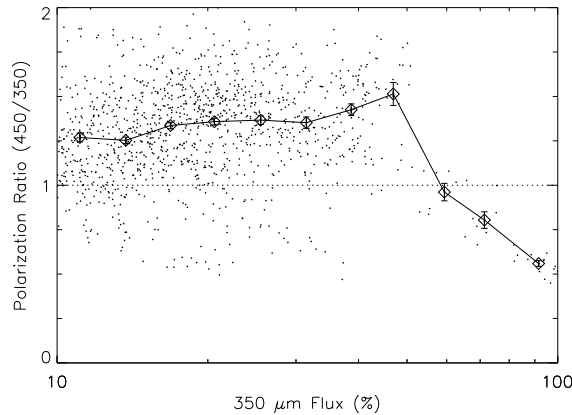


Fig. 4. Polarization ratio ( $450/350\ \mu\text{m}$ ) vs. the total  $350\ \mu\text{m}$  flux (Vaillancourt et al. 2008). Dots indicate individual measurements while diamonds represent an average over logarithmic bins of  $350\ \mu\text{m}$  flux. Error bars on the polarization ratio represent the standard deviation of the mean within each bin.

different dust components on the polarization spectrum is most obvious in high column density regions (flux  $> 50\%$  of the peak flux in Figure 4) where both the warm aligned dust and cold nearly-unaligned dust both contribute significantly to the total submillimeter emission. The polarization ratio ( $450\ \mu\text{m}/350\ \mu\text{m}$ ) changes as the relative emission contribution from the different components varies (Vaillancourt et al. 2008).

Theoretical arguments for grain alignment by radiative torques (Dolginov & Mytrophanov 1976; Draine & Weingartner 1996, 1997; Lazarian & Hoang

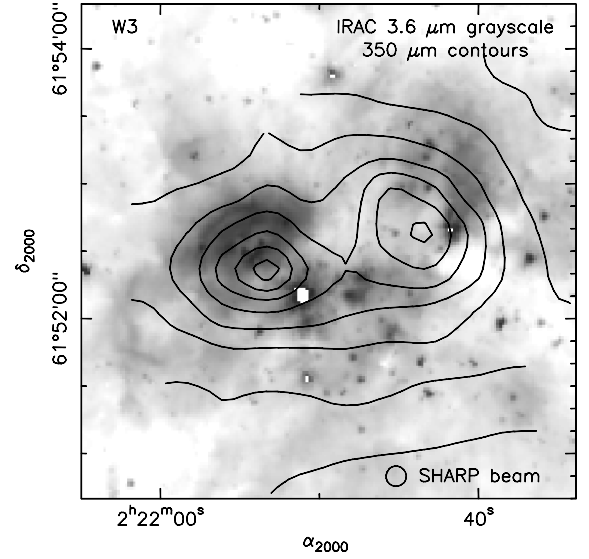


Fig. 6. W3. Contours show the total  $350\ \mu\text{m}$  flux (Schleuning 1998) while the logarithmic grayscale shows data at  $3.6\ \mu\text{m}$  from *Spitzer/IRAC* (courtesy C. D. Dowell).

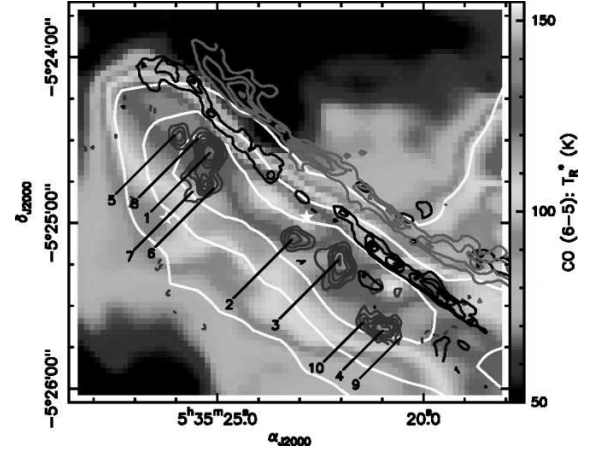


Fig. 7. Orion Bar: Clumps observed in ( $\text{H}^{13}\text{CN}$ ) emission are labeled 1–10 (Lis & Schilke 2003). White contours  $^{13}\text{CO}$  (3–2) intensity.

2007) have been confirmed by observations in the optical/near IR and FIR/SMM. Arce et al. (1998) have shown that the polarization of starlight from stars behind a molecular cloud, increases with increasing column density but only up to  $A_V \approx 1$  where the interstellar radiation field does not penetrate. In some cases the polarization increases to higher  $A_V$ , but, as pointed out by Andersson & Potter (2007), what counts is not the column density toward the observer but rather the column density between the

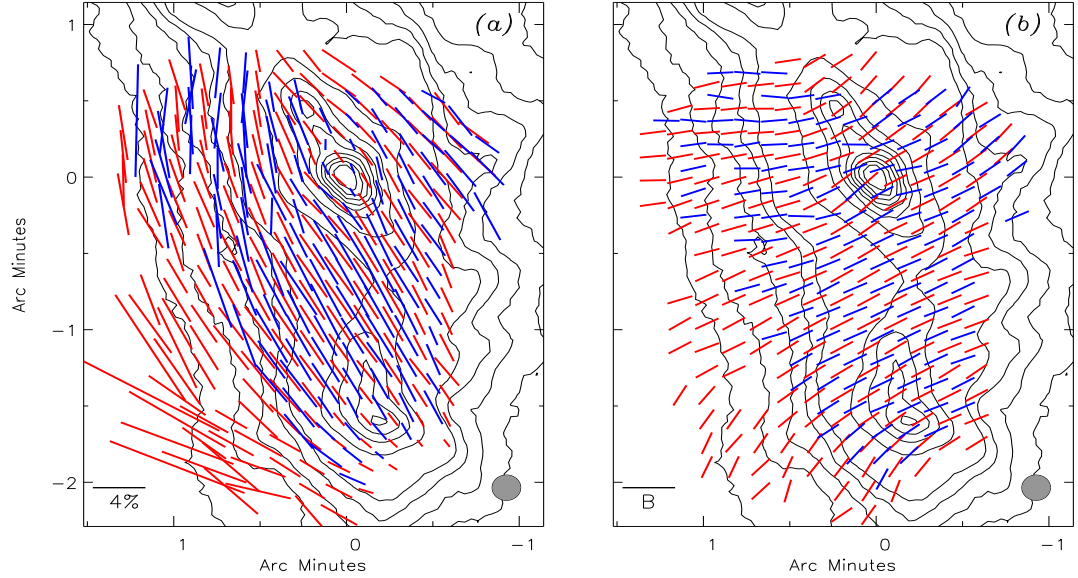


Fig. 5. Magnetic field in Orion at  $350\ \mu\text{m}$  (blue) and  $450\ \mu\text{m}$  (red). (a) Polarization vectors. (b) Same region with vectors rotated  $90^\circ$  to show orientation of the projected magnetic field Vaillancourt et al. (2008).

dust and nearby sources of radiation. Whittet et al. (2008) have shown that the polarization of starlight increases in lines of sight near embedded stars. They have further shown that the growth of ice mantles on dust grains does not inhibit grain alignment. Hence the spin-up of grains by the formation and ejection of hydrogen molecules cannot be the dominant cause of alignment.

Additional tests of alignment by radiative torques should be feasible by comparisons of polarized emission with locations of embedded star clusters and surrounding warm dust emission seen in *Spitzer* maps at  $3.6\ \mu\text{m}$  (Figure 6). Finally, the importance of radiative torques may appear in SMM polarization maps along lines of sight through dense clumps indicated by molecular lines associated with high densities (Figure 7).

The development of valid models for the magnetic field structure of molecular clouds will require high resolution multi-wavelength polarimetry at thousand of points with small beams.

### 3. SUMMARY

1. The mean magnetic fields in molecular clouds do not lie along the Galactic plane.
2. Polarization maps of Orion and DR 21 Main show evidence of gravitational collapse. The maps of flux and polarization in DR 21 Main show that the gravitational potential should dominate over magnetic support within  $\sim 1\ \text{pc}$  ( $\sim 1\ \text{arcmin}$ ) centered

on the cloud core, a region enclosing  $\sim 20,000$  solar masses.

3. The polarization spectrum of Orion, and presumably other giant molecular clouds, has a minimum near, and probably somewhat below,  $350\ \mu\text{m}$ .

4. The polarization spectrum depends on the temperatures, emissivities, and alignment efficiencies of dust grains in the various environments within the clouds.

5. A multi-wavelength photometer/polarimeter for SOFIA (Figure 8) will be uniquely suited to investigating the magnetic fields of molecular clouds (Dowell et al. 2003; Vaillancourt et al. 2007).

This work has been supported, in part, by NSF Grant AST 05-05124. Data for Figures 2, 3, 4, and 5 are from observations at the Caltech Submillimeter Observatory (CSO) with the polarimeter, SHARP (Li et al. 2008). SHARP has been supported by NSF Grants AST 02-41356, AST 05-05230, and AST 05-05124. The CSO is supported by NSF AST 05-40882. We would also like to thank Darren Dowell for providing Figures 1 and 6.

### REFERENCES

- Andersson, B.-G., & Potter, S. B. 2007, *ApJ*, 665, 369  
 Arce, H. G., Goodman, A. A., Bastien, P., Manset, N., & Sumner, M. 1998, *ApJ*, 499, L93  
 Dolginov, A. Z., & Mytrophanov, I. G. 1976, *Ap&SS*, 43, 257



Fig. 8. SOFIA in flight, 2007 May 30, from Waco Texas to its base of operations at Dryden AFB in California.

- Dowell, C. D., Davidson, J. A., Dotson, J. L., Hildebrand, R. H., Novak, G., Rennick, T. S., & Vaillancourt, J. E. 2003, *Proc. SPIE*, 4843, 250
- Draine, B. T., & Weingartner, J. C. 1996, *ApJ*, 470, 551  
 \_\_\_\_\_ . 1997, *ApJ*, 480, 633
- Heiles, C. 2000, *AJ*, 119, 923
- Hildebrand, R. H. 2002, in *Astrophysical Spectropolarimetry*, ed. J. Trujillo-Bueno, F. Moreno-Insertis, & F. Sanchez (Cambridge: Cambridge Univ. Press), 265
- Hildebrand, R. H., Dotson, J. L., Dowell, C. D., Schleuning, D. A., & Vaillancourt, J. E. 1999, *ApJ*, 516, 834
- Kirby, L. 2009, *ApJ*, 694, 1056
- Lazarian, A., & Hoang, T. 2007, *MNRAS*, 378, 910
- Li, H., Dowell, C. D., Kirby, L., Novak, G., & Vaillancourt, J. E. 2008, *Appl. Opt.*, 47, 422
- Lis, D. C., & Schilke, P. 2003, *ApJ*, 597, L145
- Mathewson, D. S., & Ford, V. L. 1970, *MmRAS*, 74, 139
- Schleuning, D. A. 1998, *ApJ*, 493, 811
- Vaillancourt, J. E., et al. 2007, *Proc. SPIE*, 6678, 9
- Vaillancourt, J. E., Dowell, C. D., Hildebrand, R. H., Kirby, L., Li, H., Novak, G., Krejny, M. M., & Houde, M. 2008, *ApJ*, 679, L25
- Whittet, D. C. B., Hough, J. H., Lazarian, A., & Hoang, T. 2008, *ApJ*, 674, 304